QUANTUM PLASMONICS

Luís Carlos Ferreira Rodrigues

Instituto Superior Técnico, Lisboa, Portugal

November 2018

ABSTRACT

In conducting materials such as metallic and semiconductor systems, coherent oscillations of collective free charge may be observed at frequencies usually in the ultraviolet spectrum. This phenomenon affects the permittivity response, which can assume negative values and allows sub-wavelength confinement of light, thus, enabling a wide range of applications. The rapid oscillations of the electron density can be quantized wherein a quantum of plasma oscillation is named plasmon. Due to this quantization, it is necessary to revise concepts of both Quantum Mechanics and the Plasmonics field. For a metal-dielectric interface, the coupling between light modes and plasmons confined at the interface gives origin to the quasi-particle surface plasmon polariton (SPP). The SPP represent the principal subject of this dissertation. The analysis of its permittivity response is performed either for the case where a local medium is assumed or for the scenario where the spatial dispersion is accounted. The quantization of the SPP electromagnetic field in the electrostatic regime is derived for both approaches. The spontaneous emission of SPP in the nonlocal approach is also subject of study for a system which consists in a two-level atom in the vicinity of a metal slab. The interaction between the atom and the SPP waves is examined, taking into account a local description of the SPP in the quasi-static approximation. Contrasts between strong and weak coupling regimes regarding the interaction of these two systems are also discussed.

Index Terms— Plasmon, Plasma Frequency, Surface Plasmon-Polariton, Charge Density Oscillation, Quantum Mechanics, Operators, Quantum Electrodynamics (QED), Harmonic Oscillator, Spontaneous Emission, Non-local Surface Plasmons

1. INTRODUCTION

The description of physical macro scale systems is typically performed by resorting to the *Newtonian laws*, which convey a simple and straightforward analysis. However, there are some interesting systems in scales of a few nanometers for which this classical approach does not convey the correct physical reality. In these systems a quantum mechanical description must be employed to accurately capture its dynamics.

Hence, this work aims to study systems within the Quantum Plasmonics [1] research field, which procures to study plasmonic systems using Quantum Mechanics. The plasmons consist in a coherent oscillation of the free density charge, that emerge at high frequencies (usually in the visible and ultraviolet spectra) in conducting materials such as metals and semiconductors [2]. The interest in this field is related with the outstanding range of possible practical applications, due to their unique characteristics, such as the subwavelength confinement and the capacity to support waves that go beyond diffraction limit [3], the spectroscopy [4] analysis, light emitters, super lenses [5] and biosensors are some of the applications explained by Plasmonics.

The plasmons may appear in different scenarios giving rise to different phenomena [6], *e.g.*, the bulk plasmons, the localized plasmons and the surface plasmon-polaritons (SPP), being the latter one of most concerns in this work.
This work proposes to study the interaction of a quantum object (*e.g.*, an atom) that is placed in the vicinity of a metal slab, which is capable of supporting SPP waves. To conduct this analysis, it is introduced the quantization of the SPP electromagnetic field in the electrostatic regime, either using a local description of the medium and one where the spatial dispersion response is considered. The coupling between these two systems can either fall into the strong or the weak regimes. Therefore, the temporal evolution of the system is examined in both regimes. In addition, is computed the probability of finding the atom in an excited and ground states over time.

As an initial approach, the problem is considered to have no loss channels and the dynamics of the system are simply obtained to solving the losses to the system through introduced in the interaction between the atom and the metal slab, since the approach developed to solve the *Schrödinger equation* for the exact *Hamiltonian* of the problem. The inclusion of losses is made heuristically by considering a term that accounts with radiation dispersed via spontaneous emission.

This paper is organized as follows. In Section 2 the main concepts of Quantum Mechanics and the quantization of the electromagnetic field are discussed. It is also introduced the description of surface plasmons (SPP) and some of its applications. Section 3 addresses the model used to describe the non-local SPP. The light-matter interactions are analyzed in Section 4, as well as the spontaneous emission of non-local

SPP. In Section 5 is mentioned the interaction in the quasi-static approximation between a two-level atom (TLA) with the metal slab (that supports local SPP). Chapter 6 is dedicated for the conclusions.

2. MAIN CONCEPTS

2.1. Quantum Mechanic Concepts

Quantum theory [7] enlightens that the state of a system can be described by a mathematical complexed valued wavefunction, generally denoted by $\psi(x,t)$, which contains all the information within a system. Also, to every physical entity (observable) a corresponding Hermitian operator exists. The wavefunction is usually described in the basis given by linear expansion of the eigenstates, which are orthogonal between each other and correspond to the measurable states of the system. The states can be represented using a bra ($\langle i|$)/ ket ($|i\rangle$) notation or by a wavefunction.

$$i\hbar\frac{d}{dt}\vec{\psi}(x,t) = \mathbf{H}\,\vec{\psi}(x,t) \tag{1}$$

The time evolution of the system is dictated by the *Schrödinger equation* given in Eq. 1. Another way to solve the dynamics of the system is using the *Heisenberg picture*, where the time evolution is comprised in the operators and not in the states (as happens in the *Schrödinger picture*).

$$H_{H.O} = \sum_{\omega_n>0}\left(\frac{1}{2}m\omega_n^2 x_n^2 + \frac{1}{2m}p_n^2\right) \tag{2}$$

In addition, the quantization of the electric field can be made by considering a cavity terminated with periodic boundary conditions [8]. This method allows to decompose the radiation fields as a sum of normal field modes, each mode associated with a unique combination between a wavenumber k and polarization n. Inspecting the energy of each electromagnetic field mode is possible to notice a clear resemblance with the energy of the quantum harmonic oscillator problem [7] given in Eq. 2, where m is the mass, ω is the frequency of the harmonic oscillator, and x and p are the position and the momentum of the system, respectively.

$$\mathbf{F} = \begin{pmatrix}\mathbf{E}\\ \mathbf{H}\end{pmatrix} = \sum_{\omega_n>0}\sqrt{\frac{\hbar\omega_n}{2}}\left(\mathbf{a_n}\mathbf{F_n}(\mathbf{r}) + \mathbf{a_n^\dagger}\mathbf{F_n^*}(\mathbf{r})\right) \tag{3}$$

Since this problem has a known solution it is made an equivalence between both problems, such that to each electromagnetic field mode an uncoupled harmonic oscillator is corresponded. Employing the creation $(\mathbf{a_n})$ and annihilation $(\mathbf{a_n^\dagger})$ operators the quantization of the electromagnetic field follows as in Eq. 3, where **E** and **H** correspond to the electric and magnetic fields and $\hbar$ is the reduced Planck constant. These bosonic operators allow to construct a solution for the eigenenrgies of the system. What is seen through the bosonic commutation relations, is that the the eigenergies for a given mode are disposed in a discrete ladder. Moreover, this ladder has an inferior eigenergy limit, corresponding to the ground state, while the upper limit is not bounded. In the ground state no photon is present, but if one applies the creation operator to this state, it is seen that the energy rises due to the emergence of one photon. Similarly, if the annihilation operator was applied to a state with n photons, the resulting system would contain $n-1$ photons.

This quantization is only valid for non-dispersive media, and for the dispersive, a different normalization needs to be employed, as discussed further.

2.2. Plasmonics

2.2.1. Drude's Model

In good conductors, for energies near the *Fermi level*, a coherent motion of the free electrons is observed [6]. The plasmon is the quantum of free electrons oscillation waves, and may be perceived as a collection of electrons, which is described as a quasiparticle with discrete energy, identical to a photon for electromagnetic oscillations. Although one should use a quantum model to characterize the system, almost all the important properties can be unveiled with a classical free electron model.

This phenomenon emerges in different circumstances, such as volume plasmons, surface plasmon polaritons, local

$$\varepsilon_m = 1 - \frac{\omega_p^2}{\omega^2 - i\omega\gamma}, \tag{4}$$

In order to study the plasmons behavior, it is crucial to capture the free electrons response (permittivity) in metals to an external electric field. This can be attained by using the *Drude's* model, which is a particular case of *Lorentz* model with no restoring force (since the electrons are free). This model describes the motion, in a metal, of the electron "gas" moving against a background of heavy immobile ions using the Newton laws of motion. The relative permittivity formula is then obtained and can be found in Eq. 4, where ω_p corresponds to the plasma frequency, ω is the frequency and γ is the damping rate, which accounts with the material losses.

$$\omega = \sqrt{c^2k^2 + \omega_p^2} \tag{5}$$

The dispersion equation, given in Eq. 5, shows that for frequencies above the plasma frequency the system comports transversal propagation modes and for frequencies near the plasma frequency longitudinal modes (for a thorough analysis consult [9]). The longitudinal wave corresponds to having $\epsilon_m = 0$.

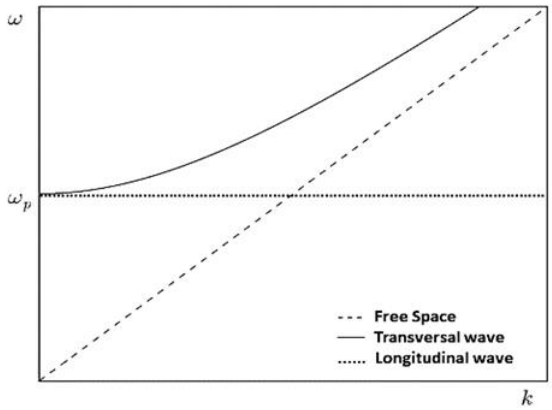

Figure 1: Dispersion of k for Drude's model containing the transversal and longitudinal propagation modes.

2.2.1. Surface Plasmons

The surface plasmon polaritons or simply surface plasmons are defined as the quanta of coupled oscillations between plasmons and polaritons (*i.e.*, polarization waves from a dielectric) and are extremely confined on the interface between a metal and a dielectric as represented in Figure 2. Moreover, this coupling is mediated by an electromagnetic field. To analyze the dispersion of the SPP wave [10] one must solve *Maxwell equations* at the metal-dielectric interface for a solution that is supported without external excitation. The surface plasmon wave is characterized by a TM, which must exponentially decay along $\vec{z}$ either to above or below the interface, since the wave is highly confined to the interface.

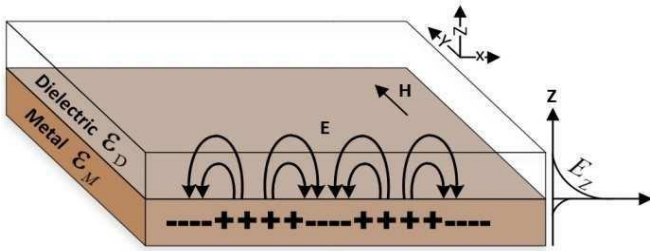

Figure 2: Dielectric-metal interface scheme with SPP propagation [11].

$$k_x = \frac{\omega}{c}\sqrt{\frac{\varepsilon_d \varepsilon_m}{\varepsilon_d + \varepsilon_m}} \qquad (6)$$

By boundary conditions inspection it may be verified the dispersion relation in Eq. 6 and that such propagations occur only if ε_m (metal permittivity) and ϵ_d (dielectric permittivity) must have opposite signals [12]. Thus ε_m must be negative and imposing a non-evanescent k_x mode, it follows that the only possible solution exists for $\varepsilon_m(\omega) < -\varepsilon_d(\omega)$. The upper allowed frequency is obtained for $\varepsilon_d + \varepsilon_m(\omega_{spp}) = 0$, which neglecting the damping term γ leads to the surface plasmon frequency $\omega_{sp} = \frac{\omega_p}{\sqrt{1+\varepsilon_d}}$. Figure 3 shows the dispersion curves for the surface plasmons in contrast to the bulk plasmon's and the free space dispersion.

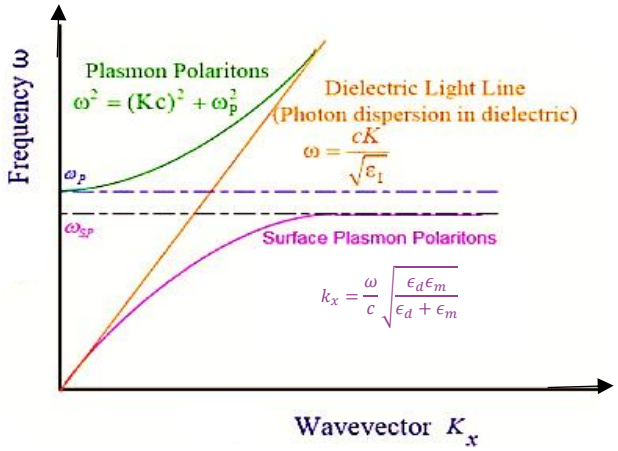

Figure 3: Dispersion curves for photons, bulk plasmons and surface plasmons, where for the surface plasmons the convergence frequency is ω_{sp} [11].

The SPP wavevector is always greater than the photon wavevector in the dielectric, which means that the surface plasmon cannot be excited through direct incident radiation. This can be overcome by radiating through a material (e.g. a prism) with a higher refraction index in a *Kretschmann* or *Otto configuration* [13].

2.2.1. Plasmonic Applications

The local plasmons are metal nanoparticles its behavior is identical to the discussed for volume. Moreover, its resonant scattering power is sensible to dielectric constant changes of the environment which allows their usage in biological and chemical sensing and detection applications [13]. Therefore, by inserting metal nanoparticles into a biological sample, it is possible to measure the occurred shifts on the resonance frequency associated with certain chemicals and molecules. In addition, surface plasmon sensors are also a viable option to detect environmental changes for very short distances from the surface interface [14].

Another possible application of plasmons lies on *Raman scattering spectroscopy*[14], used to identify the chemical composition of a sample since the molecular vibrations energy spectrum provide a fingerprint-like characteristic. The *Raman scattering effect* is analogous to a FM modulation, where a monochromatic light behaves like a carrier and is modulated by the molecular vibrations (phonons). This process results in scattered radiation that suffers a frequency shift correspondent to the frequencies associated with the molecular oscillations. The uniqueness of the originated spectrum is related to the dependence of the molecular vibrations in its particular molecular structure (for a detailed description consult [15]).

3. NON-LOCAL SURFACE PLASMONS

The description of the plasmonic response assuming a homogeneous charge distribution along the metal slab is not always the most adequate approach due to the outmatching results when compared with the experimental ones [16]. Mechanisms such as the motion of single electrons and the repulsive Coulomb interactions between each other should be considered. These interactions provoke diffusion effects, which create a repelled motion of electrons from the areas with higher charge concentration [17], [18]. An immediate implication of this charge nonlocality is that the value of the electric polarization in a specific position (due to an external electric field) is no longer solely determined by the response of that point, but also of its surrounding region. Consequently, this implies the introduction of a new electron's motion model for nonlocal media and the derivation of a dielectric spatial dispersive response [19].
A description for the permittivity response may be accomplished by using the *Hydrodynamic* model [16], [20].

$$\varepsilon(k,\omega)=\varepsilon_0\left[\mathrm{I}-\frac{\omega_p^{\,2}}{\omega(\omega+i\gamma)}\left[\mathrm{I}-\frac{\vec{k}\otimes\vec{k}}{k^2-\frac{\omega(\omega+i\gamma)}{\beta^2}}\right]\right] \tag{7}$$

The phenomenological parameter β is introduced in this model to account with the diffusion effects and the derived permittivity follows as in Eq. 7, where $\varepsilon_0$is the vacuum permittivity.

$$k_{\perp,I}=\pm\sqrt{k_x^{\,2}+k_y^{\,2}+\frac{\frac{\omega_p^{\,2}}{\varepsilon_\infty}-\omega(\omega+i\gamma)}{\beta^2}} \tag{8}$$

Analyzing the *Maxwell equations* is possible to infer that the wave modes of this system can either be transverse or longitudinal. The wavevector for the former wave is $k_{\parallel}=\sqrt{k_x^2+k_y^2}$ and for the latter is given in Eq. 8.

$$\phi(r,t)=e^{i(k_{\parallel}x-\omega t)}\begin{cases}A_1e^{k_{\perp}z}+A_2e^{k_{\perp,I}z} & ,z<0\\ Be^{-k_{\perp}z} & ,z>0\end{cases} \tag{9}$$

Considering the fields in the electrostatic regime it is possible to obtain write the electric field as the gradient of a scalar electric potential. Solving the *Gauss's law* for no external charges is achieved the structure of the potential written in Eq. 9, where A_1, A_2 and B are normalization constants.

Furthermore, to obtain the dispersion relation, it no longer suffices to use the *Maxwellian Boundary Conditions*, because the nonlocality introduces a new degree of freedom in the material response. Then, it an *Additional Boundary Condition* (ABC) needs to be chosen. The ABC choice is the same found at [21], which is $\vec{J}\,|_{z=0}\,.\,\hat{n}=0$.

$$k_{\perp}=\frac{|\omega|}{\beta}\left(1-\frac{\omega_{sp}^2}{\omega^2}\right) \tag{10}$$

The dispersion equation obtained is presented in Eq. 10 and its plot is illustrated in Figure 4. As one may confirm the nonlocalities introduce a slight slope in the dispersion relation graphic, which implies that for frequencies above the surface plasmon resonance (ω_{sp}) the propagation of waves is possible, in contrast to the local scenario in the quasi-static approximation.

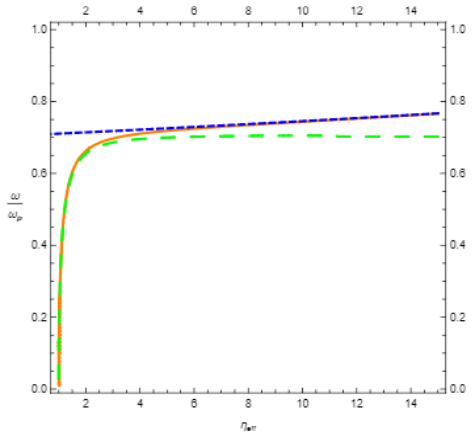

Figure 4: Lossless Surface Plasmon dispersion curves with $\beta/c = 100$ where c is the speed of light. The green dashed curve corresponds to local scenario within the Drude model, the orange curve corresponds to nonlocal medium without approximations, the blue dashed curve corresponds to nonlocal medium in the electrostatic regime.

$$n_{sp}(\omega)=\frac{\omega^4-\omega_{sp}^{\,4}}{2\pi\beta^2\omega^3} \tag{11}$$

The density of states (DOS) [22] for the non-local SPP is also derived, using the periodic boundary conditions method and the formula acquired is in Eq. 11. In *Figure 5* is plotted the DOS, from where is seen that the states are distributed for frequencies above ω_{sp}, unlike to the SPP in the electrostatic regime, where the DOS is all concentrated at ω_{sp}.

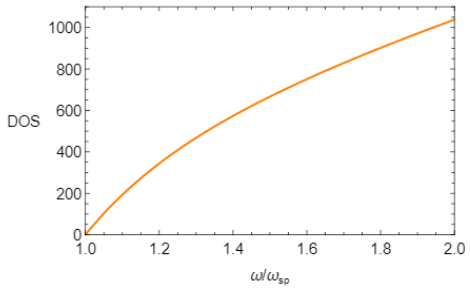

Figure 5: Density of States of a Nonlocal Surface Plasmon, which is plotted for the frequencies in the vicinity of the surface plasmon resonance. The frequency is normalized in relation to ω_{sp}.

4. QUANTUM MODEL DESCRIPTION OF LIGHT-MATTER SYSTEMS

The two-level approximation model [23] is the elected approach to take in quantum optics when dealing with atom-light interactions, since it reproduces the important features [24] of the system such as *Spontaneous Emission* [25] and the *Rabi oscillations* [26]. This approximation considers that the real structure of an atom, containing infinite number of energy levels, can be well described at some extent by one having only two energy levels [23]. This approximation is supported by two other considerations [27], the *Dipole Approximation* (where its derivation is found at [7]) and the assumption that an external field has a near resonance frequency in relation to the atomic frequency ω_0 associated with the energy gap between these two atomic levels[28]. This last assumption is related with the *Rotating Wave Approximation* (RWA) [29], that for the case of radiation interaction, considers that the frequencies that are near ω_0 contribute more for the transitions between states.

$$H_{At} = E_e |e\rangle\langle e| + E_g |g\rangle\langle g| \tag{12}$$

The *Hamiltonian* used to represent the TLA is given in Eq. 12, where E_e and E_g are the energies of the excited ($|e\rangle$) and ground ($|g\rangle$) states, respectively. Also, the operators σ^+ and σ^- are introduced. When σ^+ is applied to $|g\rangle$, is yields to $|e\rangle$ and if σ^- is applied to $|e\rangle$ then the ground state is obtained.

$$\mathbf{H}_{Tot} = \mathbf{H}_{At} + \mathbf{H}_{EM} - \vec{\boldsymbol{\mu}} \cdot \vec{\mathbf{E}}(r_0, t) \tag{13}$$

In order to compute the spontaneous emission for the system formed by the TLA placed above the non-local metal slab, is necessary to the address the *Hamiltonian* of this system, that is determined in Eq. 13. This *Hamiltonian* is derived [7][30] in the *Dipole Approximation*. The last term on the right side of the equation represents the interaction between the two unperturbed systems (TLA and metal slab), where $\vec{\boldsymbol{\mu}}$ is the electric dipole moment.

$$\Gamma_{sp}(\omega) = \frac{k_0^3 L^2 \omega_0}{\hbar} \frac{|\gamma|^2 |B|^2 e^{-2k_0 r_0}}{\left| -\beta + \dfrac{k_0 \beta^2}{\sqrt{k_0^2 \beta^2 + 4\omega_{sp}^2}} \right|} \tag{14}$$

Moreover, it is also resorted to the *Golden Fermi Rule* [31] to compute the emission rate Γ for the non-local SPP, whose expression may be seen in Eq. 14, where L is the length of the slab sides, γ is the element of the electric dipole moment matrix, r_0 is the distance between the two systems and k_0 is the wave vector of the non-local SPP for which is obtained a frequency equal to ω_0. The plot of the emission rate for different values of β is given in the Figure 6. As one may infer, the at $\omega = \omega_{sp}$ the emission rate is zero due to its dispersion relation ($k_{\parallel}(\omega_{sp}) = 0$). In addition, as we enter in the local limit, Γ regains the form of a *Dirac delta* that is obtained for the local response of the SPP in the quasi-static approximation.

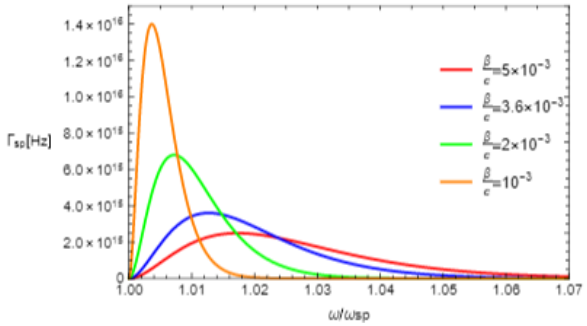

Figure 6: The graphic shows the plot of the Emission rate of the SPP in a non-local silver slab, for different values β . The red, blue, green and orange curves correspond to diffusion strengths of $\frac{\beta}{c} = 5 \times 10^{-3}$, $\frac{\beta}{c} = 3.6 \times 10^{-3}$, $\frac{\beta}{c} = 2 \times 10^{-3}$ and $\frac{\beta}{c} = 10^{-3}$, respectively.

The comparison of Γ_{sp} with the emission rate in free space is also discussed, for which it is verified that in the absence of the metal slab (free space) the emission rates are much lower, and in specific Γ_{sp} can achieve values 8000 times higher.

5. QUANTUM INTERACTION

The interaction that emerges between a TLA and local SPP, when placing the atom near a metal slab is examined in the electrostatic regime. Moreover, it is pretended to observe what are the possible states of the system and how its probability over the time evolves. It is assumed that the initial state is $|e, 0\rangle$ (where the right-side number corresponds to the number of photons in that state).

The interaction between a quantum object and a quantized electromagnetic field imposes greats difficulties due to the

treatment of the infinite modes that appear. Therefore, it is usual to consider the interaction of multi-level atoms with a few modes of the quantized radiation field [26][27]. These matter-bosonic interactions usually dispose of the Jaynes–Cummings model [34], which gives the structure of the *Hamiltonian* for these interactions. However, this model uses the RWA, which does not allow the inclusion of strong coupling regimes.

$$\mathbf{H} = \frac{\hbar\omega_{sp}}{2}\hat{\mathbf{c}}^{\dagger}\hat{\mathbf{c}} + \frac{\hbar\omega_0}{2}\boldsymbol{\sigma}_z - (g\boldsymbol{\sigma}^{+} + g^{*}\boldsymbol{\sigma}^{-})\left(\hat{\mathbf{c}} + \hat{\mathbf{c}}^{\dagger}\right) \quad (15)$$

Then, it was used the exact *Hamiltonian* already presented (in Eq. 13) in order to study the strong coupling regime. The problem of the radiation infinite modes can be circumvented by reformulating the *Hamiltonian* of the system in such a way that an analytical solution may be extracted. This formulation is only possible because it is considered the local description of the SPP in the electrostatic regime, since that all the wave modes are associated with the same frequency ω_{sp}. This degeneracy in the frequency makes possible this *Hamiltonian* reformulation, which results in Eq. 15, where $g = \gamma^{*}\sqrt{\frac{\hbar\omega_{sp}}{32\pi\varepsilon_0 r_0^3}}$ gives the strength of the coupling, and the normalized operators $\hat{\boldsymbol{c}}^{\dagger}$and $\hat{\boldsymbol{c}}$ are similar to the bosonic operators. Afterwards, a general wavefunction spanned in the eigenbasis of the unperturbed systems is used to solve the *Schrödinger Equation*. Moreover, the time evolutions of both unperturbed systems are included in this general wavefunction, which contains also a coefficient (time dependent) to comprise the evolution of the perturbation.

$$\dot{c}_n(t) = g\frac{i}{\hbar}e^{i\omega_0 t}\left(\tilde{c}_{n-1}(t)\sqrt{2n}e^{i\omega_{sp}t} + \tilde{c}_n(t)\sqrt{2n+1}e^{-i\omega_{sp}t}\right) \quad (16)$$

$$\dot{\tilde{c}}_n(t) = g^{*}\frac{i}{\hbar}e^{-i\omega_0 t}\left(c_n(t)\sqrt{2n+1}e^{i\omega_{sp}t} + c_{n+1}(t)\sqrt{2n+2}e^{-i\omega_{sp}t}\right) \quad (17)$$

By applying the *Hamiltonian* to the initial state $|e,0\rangle$ is seen that the only new state that appears is $|g,1\rangle$. If this process is repeated iteratively one may notice that the only states that are obtained are $|e,2n\rangle$ and $|g,2n+1\rangle$ for $n \in \mathbb{N}$. This means that the system can only have even number of photons and be in the excited states simultaneously or be in the ground state and have an odd number of photons. Hence, the *Schrödinger Equation* leads to the system of the linear differential equations given in Eq. 16 and Eq. 17. Using a truncation for the coefficients enables the computation of a solution.

Therefore, the probabilities of the states in the excited ($P_e(t)$) and ground ($P_g(t)$) atomic state is plotted for two different regimes: the weak coupling regime (in Figure 7) and the strong one (Figure 8). As one may verify, the rate of the oscillations in the strong coupling is much higher than the one in the weak regime. Moreover, is seen that fir the weak coupling the oscillations are smooth while for the other regime the variations are more abrupt. This is explained through the interference provoked by the frequency spectrum of each individual state when combined.

In fact, for the strong coupling regime the number states with significant probability of being excited is higher in comparison to the weak regime. This implies that the number of states needed to reproduce accurately the system dynamics is also higher. Indeed, in the weak coupling scenario, besides the two first coefficients all the other states may be neglected whilst having a good representation of the system. This explains why the RWA should only be used in the weak regime.

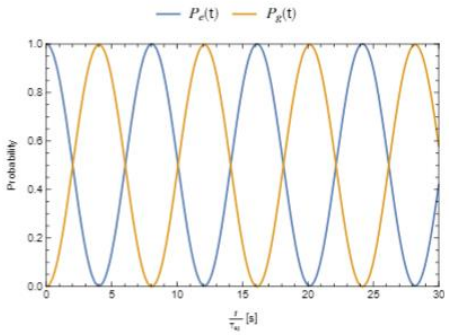

Figure 7:Plots of the probabilities $\mathrm{P_e(t)}$ (orange curve) and $\mathrm{P_g(t)}$ (blue curve), for a distance $\mathrm{r_0 = 10}$ nm and considering a Rydberg atom with $\gamma = 1212 \times 10^{-30}$ C. m.

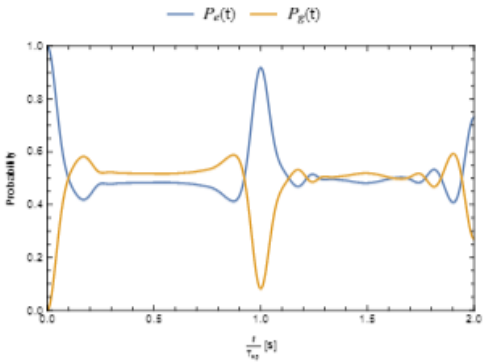

Figure 8: Plots of the probabilities $\mathrm{P_e(t)}$ (orange curve) and $\mathrm{P_g(t)}$ (blue curve), for a distance $\mathrm{r_0 = 1}$ nm and considering a Rydberg atom with $\gamma = 1212 \times 10^{-30}$ C. m

To corroborate these affirmations, is plotted the probability of the third and fourth coefficient for the case of weak (Figure 9) and strong (Figure 10) coupling, to see for each of the cases its contribution is relevant.

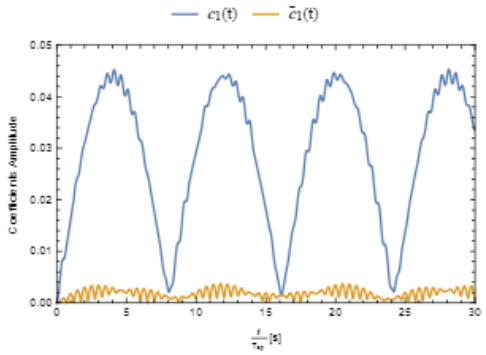

Figure 9: Plots of the probabilities $|c_1(t)|^2$ (orange curve) and $|\tilde{c}_1(t)|^2$ (blue curve), for a distance $r_0 = 10$ nm and considering a Rydberg atom with $\gamma = 1212 \times 10^{-30}$ C. m

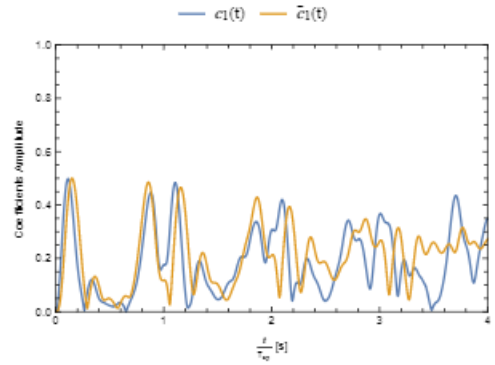

Figure 10: Plots of the probabilities $|c_1(t)|^2$ (orange curve) and $|\tilde{c}_1(t)|^2$ (blue curve), for a distance $r_0 = 1$ nm and considering a Rydberg atom with $\gamma = 1212 \times 10^{-30}$ C. m

The study of this interaction accounting with losses is also conducted, where the losses come from the spontaneous emission phenomenon. Hence, it is used the emission rate to define a new phenomenological frequency $\omega_0'' = \frac{\Gamma}{2}$. The procedure to include the losses is by solving the system in the lossless regime and afterwards multiply the coefficients by $e^{-\omega_0'' t}$. This study is divided in the strong and weak coupling, where the used emission rates were 20THz and 800 THz, respectively. As is seen in Figure 11 for the weak coupling and in Figure 12 for the strong coupling, the probabilities $P_e(t)$ and $P_g(t)$ present more oscillations for the weak regime, before all the energy is dispersed. Since the only parameter that was altered was the distance r_0 in the calculation of $\tilde{g}$ and the emission rate, then this implies that the variation of the emission rate is stronger than the variation of $\tilde{g}$. Indeed, the emission rate increases exponentially with the decreasing of the distance, while that $\tilde{g}$only increases with a magnitude of $3/2$.

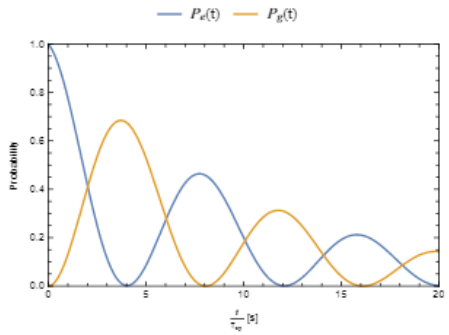

Figure 11: Plots of the probabilities $P_e(t)$(blue curve) and $P_g(t)$ (orange curve), in the weak coupling regime ($r_0 = 10$ nm and $\Gamma =$ 20THz. It was used $\gamma = 100 \times 10^{-30}$ C. m.

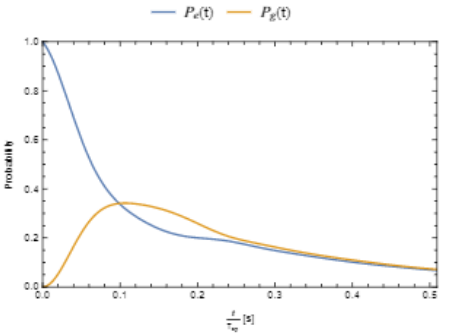

Figure 12: Plots of the probabilities $P_e(t)$(blue curve) and $P_g(t)$ (orange curve), in the weak coupling regime ($r_0 = 1$ nm and $\Gamma =$ 20THz. It was used $\gamma = 100 \times 10^{-30}$ C. m

6. CONCLUSIONS

The purpose of this report was to study the interaction between a TLA and SPP, where the former is placed in the vicinity of the metal slab, which supports SPP waves. To accomplish this objective, it was assumed a local response of the metal slab and the quasi-static approximation for the system.

Another parallel objective for this work was to comprehend how the introduction of the nonlocality in the permittivity response of the SPP affects its propagation and, in specific, its dispersion relation. This analysis is made in comparison with the analogous local response, where for the sake of simplicity is considered the electrostatic regime in both scenarios. The study of the interaction between the TLA and the SPP waves was performed by analyzing the two systems individually as an initial approach.

About the quantization of the electromagnetic field, is seen that, for each radiation mode, a quantum harmonic oscillator can be associated. Moreover, the introduction of the bosonic operators leads to a discrete set of eigenenergies that are equally spaced and present a lower bound designated by ground state. In addition, the quantization of the surface plasmon is possible due to the quasi-particle feature involving

these collective charge oscillations. Nevertheless, the quantization of the SPP in the local model is different from the one with spatial dispersion. However, the main difference lies on the normalization of the eigenmodes, where different formulas are used.

For the spatial dispersive SPP, the diffusion effects are included in the permittivity via the phenomenological parameter β and using the *Hidrodynamic model*. This nonlocality means that the response of the permittivity in a given point depends not only of its response in that point but also in its surrounding region. The difficulty on the analysis of the system is surpassed by considering a solution formed by the sum of planar waves in the *k* domain. Consequently, the permittivity acquires a dependence on the wave vector and it may be expressed as sum of a longitudinal and transverse permittivity. From Eq. 7, one may notice that the spatial dispersion only affects the longitudinal component. Also, through the *Gauss's law*, an additional wave solution is observed, which is obtained by making this longitudinal component equal to zero.

To obtain the dispersion relation for the non-local SPP is necessary to use an *ABC* besides the habitual *Maxwellian* boundary conditions. This additional condition emerges due to the new degrees of freedom that arise in the medium due to its non-homogeneity. A usual procedure to resolve the arbitrariness in the ABC choice is using constraints (with physical meaning) either for the charge density or the current.

Regarding the dispersion relation for the spatial dispersive medium in the quasi-static regime, it is seen that the value of ω is not constant for all the wavenumbers, in opposition to what happens in the local analogous. Also, in the latter the only frequency that supports waves is ω_{sp}. The monotonic curve of the non-local SPPs presents a slight positive slope, and the null wavevector is observed at $\omega = \omega_{sp}$, consequently implying that the propagation is made for frequencies above the surface plasmon resonance. By the dispersion formula one can deduce that if β increases, so does the slope of the curve. The computation of the DOS for the non-local SPP confirms that the infinite number of states found for the local model (given by $\sim \delta(\omega - \omega_{sp})$) is redistributed over frequencies above ω_{sp}.

Regarding the atom description, in this study was employed the simplification of the TLA in order to quantize the atom. In this approximation, is assumed that the only relevant eigenenergies are the ground state and the one immediately above in terms of energy. The arguments that support this approximation lie on the consideration that an external radiation field must have a frequency close to the atomic frequency relatively to these two states considered. Moreover, the frequency of the radiation must be detuned from frequencies associated with the neglected atomic levels. It was also considered the *Dipole Approximation*, which states that for wavelengths of the electric field much larger than the atomic dimensions, the field can be said constant over the atom's region.

The solutions for the problem proposed was solved in a basis formed by the tensorial product of the eigenstates of the unperturbed systems TLA and local SPP. In addition, it was considered that the solutions of the new system could be obtained by incorporating the time evolution of the unperturbed systems in the solution. The incorporation of the $\widehat{\mathbf{H}}_{\mathbf{Int}}$ time evolution is done by including an additional coefficient (time dependent). This problem in the electrostatic regime gives origin to a system of differential linear equations that may be solved using the truncation of the coefficients above a chosen number. Also, the solutions of the system, given the initial state $|e,0\rangle$, are of the form $|e,2n\rangle$ and $|g,2n+1\rangle$ ($n \in \mathbb{N}$). Thus, the only states that can appear in this system in the atomic excited state correspond to states having an even number of photons and being simultaneously in the ground state. This solution would be inverted if the initial state was$|g,0\rangle$.

The solutions obtained were evaluated in the weak and strong coupling regimes. The main conclusion that is extracted for the weak regime in resonance ($\omega = \omega_{sp}$) is that the number of states relevant to describe the dynamics of the interaction are mainly $|e,0\rangle$ and $|g,1\rangle$, which means that the system presents adversities to transit to the above states. Because of the small interference with higher states, the oscillation in the probabilities $P_e(t)$) and $P_g(t)$ are smooth and similar to the sinusoidal *Rabi oscillations*, addressed for the classical described radiation wave. Hence, the *RWA* represents a good approximation in these conditions.

However, in the strong coupling at the resonance, the number of coefficients, whose contribution entails most of the system evolution, is superior to the one found in the weak coupling regime. Also, the probability of each state oscillated much faster is higher in this regime (strong coupling). The contribution of more states explains why the probabilities $P_e(t)$ and $P_g(t)$ have a non-smooth variation over the time, since the sum of the different frequency spectra for each state will cause interference effects. For this case, the *RWA* exhibits large discrepancies when compared to the real solution.

The interaction accounting with channel losses is also examined, where its inclusion is done through the emission rate phenomenon. The latter is derived using the *Fermi Golden Rule*, which consists in the first order term of the *Time Dependent Perturbation Theory*. Furthermore, it was also employed the *RWA* in order to keep the terms of $\widehat{\mathbf{H}}_{\mathbf{Int}}$ that are associated with energy conservation. The results of the emission rate for the non-local SPP show a peak for frequencies near the surface plasmon resonance. The effect of the spatial dispersion in the emission rate is that for larger diffusion effect, the peak becomes wider and its maximum amplitude decreases. Therefore, in the local limit is possible to infer that the emission rate obtained will become a Dirac delta, which is in concordance to the local result.

In conclusion, the spatial dispersive response allows to frequencies above the ω_{sp} to support wave modes, which is intimately linked with the new longitudinal wave solution that appears for $\varepsilon_L(\omega, \vec{k}) = 0$. On the other hand, this implies that the DOS in the non-local case is redistributed over a wider interval of frequencies and consequently the emission rate at ω_{sp} is no longer given by a result proportional to $\delta(\omega - \omega_{sp})$.

For future work, it may be developed a more accurate description of the spatial dispersion for the surface plasmons, *e.g.*, using other terms [35] that enable a better fit to the experimental data. Also, the study of the interaction of this plasmonic apparatus with a more interesting and complex system may be taken, like a multi-level atom with a degree higher than two. Then, a discussion about the dynamics of the new system in strong and weak coupling, as well as contrasting results with the TLA, should be extended.

Another development that could be made is the inclusion of other loss channels besides the ones already considered due to the emission rate. For example, it could be accounted the energy that is dispersed in the medium, which was initially introduced by the damping term in the permittivity. This introduction would need to be done in a heuristically way since the losses usually imply that the system's *Hamiltonian* loses its Hermitian property.

The interaction between the SPP waves and the TLA described in this dissertation, but for the case where the medium has an anisotropic response, could also lead to an interesting problem.

8. REFERENCES

[1] J. M. Fitzgerald, P. Narang, R. V. Craster, S. A. Maier, and V. Giannini, "Quantum Plasmonics," *Proc. IEEE*, vol. 104, no. 12, pp. 2307–2322, Dec. 2016.

[2] Y. Li, *Plasmonic optics: theory and applications*. Bellingham, Washington: SPIE Press, 2017.

[3] M. S. Tame, K. R. McEnery, Ş. K. Özdemir, J. Lee, S. A. Maier, and M. S. Kim, "Quantum plasmonics," *Nat. Phys.*, vol. 9, p. 329, Jun. 2013.

[4] S. G. Patching, "Surface plasmon resonance spectroscopy for characterisation of membrane protein–ligand interactions and its potential for drug discovery," *Biochim. Biophys. Acta BBA - Biomembr.*, vol. 1838, no. 1, pp. 43–55, Jan. 2014.

[5] Y. Fu, J. Wang, and D. Zhang, "Plasmonic Lenses," in *Plasmonics - Principles and Applications*, K. Y. Kim, Ed. InTech, 2012.

[6] M. Silveirinha, "Lecture Notes of Nano-Elecctromagnetic Plasmonics and Materials," Coimbra, Dec-2015.

[7] R. Shankar, *Principles of quantum mechanics*, 2nd ed. Springer.

[8] M. G. Silveirinha, "Quantization of the electromagnetic field in nondispersive polarizable moving media above the Cherenkov threshold," *Phys Rev A*, vol. 88, no. 4, p. 043846, Oct. 2013.

[9] I. Hutchinson, "Chapter 5 Electromagnetic Waves in Plasmas." 2003.

[10] L. Novotny and B. Hecht, *Principles of Nano-Optics*. Cambridge: Cambridge University Press, 2006.

[11] R. Sadaf Anwar, H. Ning, and L.-F. Mao, *Recent advancements in surface plasmon polaritons- plasmonics in subwavelength structures at microwave and terahertz regime*. 2017.

[12] B. Ung and Y. Sheng, "Interference of surface waves in a metallic nanoslit," *Opt Express*, vol. 15, no. 3, pp. 1182–1190, Feb. 2007.

[13] O. Benson, "Elements of Nanophotonics," Humboldt-Universität zu Berlin, 29-May-2009.

[14] "Surface plasmons," ETH Zurich.

[15] F. Schwabl, *Advanced Quantum Mechanics*, 2nd Edition. Springer Science & Business Media, 2013.

[16] M. Moeferdt, "Nonlocal and Nonlinear Properties of Plasmonic Nanostructures Within the Hydrodynamic Drude Model," PhD Thesis, Humboldt-Universität zu Berlin, Mathematisch-Naturwissenschaftliche Fakultät, 2017.

[17] Y. Luo, A. I. Fernandez-Dominguez, A. Wiener, S. A. Maier, and J. B. Pendry, "Surface Plasmons and Nonlocality: A Simple Model," *Phys. Rev. Lett.*, vol. 111, no. 9, Aug. 2013.

[18] C. David, "Two-fluid, hydrodynamic model for spherical electrolyte systems," *Sci. Rep.*, vol. 8, no. 1, Dec. 2018.

[19] R.-L. Chern, "Spatial dispersion and nonlocal effective permittivity for periodic layered metamaterials," *Opt Express*, vol. 21, no. 14, pp. 16514–16527, Jul. 2013.

[20] G. Barton, "Some surface effects in the hydrodynamic model of metals," *Rep. Prog. Phys.*, vol. 42, no. 6, pp. 963–1016, Jun. 1979.

[21] C. Schwartz and W. L. Schaich, "Hydrodynamic models of surface plasmons," *Phys. Rev. B*, vol. 26, no. 12, pp. 7008–7011, Dec. 1982.

[22] R. Carminati *et al.*, "Electromagnetic density of states in complex plasmonic systems," *Surf. Sci. Rep.*, vol. 70, no. 1, pp. 1–41, Mar. 2015.

[23] W. W. Chow, S. W. Koch, and M. Sargent, *Semiconductor-Laser Physics*. Berlin, Heidelberg: Springer Berlin Heidelberg, 1994.

[24] R. W. Boyd, *Nonlinear optics*, 3rd ed. Amsterdam ; Boston: Academic Press, 2008.

[25] H. Yokoyama and K. Ujihara, Eds., *Spontaneous emission and laser oscillation in microcavities*. Boca Raton: CRC Press, 1995.

[26] K. A. Fischer, L. Hanschke, M. Kremser, J. J. Finley, K. Müller, and J. Vučković, "Pulsed Rabi oscillations in quantum two-level systems: beyond the area theorem," *Quantum Sci. Technol.*, vol. 3, no. 1, p. 014006, Jan. 2018.

[27] M. Frasca, "A modern review of the two-level approximation," *Ann. Phys.*, vol. 306, no. 2, pp. 193–208, Aug. 2003.

[28] L. Allen and J. H. Eberly, *Optical Resonance and Two-Level Atoms*. Dover Publications, 2012.
[29] K. Fujii, “Introduction to the Rotating Wave Approximation (RWA) : Two Coherent Oscillations,” *ArXiv13013585 Math-Ph Physicsquant-Ph*, Jan. 2013.
[30] M. O. Scully and M. S. Zubairy, *Quantum optics*. Cambridge: Cambridge University Press, 1997.
[31] J. M. Zhang and Y. Liu, “Fermi’s golden rule: its derivation and breakdown by an ideal model,” *Eur. J. Phys.*, vol. 37, no. 6, p. 065406, Nov. 2016.
[32] A. Messina, S. Maniscalco, and A. Napoli, “Interaction of bimodal fields with few-level atoms in cavities and traps,” *J. Mod. Opt.*, vol. 50, no. 1, pp. 1–49, Jan. 2003.
[33] G. Benivegna and A. Messina, “Collective behavior of *M* bosonic modes interacting with a single two-level atom,” *Phys. Rev. A*, vol. 37, no. 12, pp. 4747–4751, Jun. 1988.
[34] E. T. Jaynes and F. W. Cummings, “Comparison of quantum and semiclassical radiation theories with application to the beam maser,” *Proc. IEEE*, vol. 51, no. 1, pp. 89–109, 1963.
[35] A. Archambault, F. Marquier, J.-J. Greffet, and C. Arnold, “Quantum theory of spontaneous and stimulated emission of surface plasmons,” *Phys. Rev. B*, vol. 82, no. 3, Jul. 2010.